Preceramic Polymer Blends as Precursors for Boron-Carbide/Silicon-Carbide Composite Ceramics and Ceramic Fibers

Marta M. Guron,[†] Xiaolan Wei,[†] Daniel Welna,[‡] Nicholas Krogman,[‡] Myung Jong Kim,[†] Harry Allcock,[‡,*] and Larry G. Sneddon[†,*]

Department of Chemistry, University of Pennsylvania, Philadelphia, Pennsylvania 19104-6323, and Department of Chemistry, The Pennsylvania State University, University Park, Pennsylvania 16802

Received February 2, 2009. Revised Manuscript Received March 5, 2009

Simple blends of the poly(norbornenyldecaborane) (PND) boron-carbide preceramic polymer with either of the commercial poly(methylcarbosilane) (PMCS) or allylhydridopolycarbosilane (AHPCS) silicon-carbide preceramic polymers have been found to provide excellent processable precursors to boron-carbide/silicon-carbide ceramic composite materials. The blends exhibited good char yields with tunable ceramic compositions. Certain compositions of the PND/AHPCS derived ceramics also exhibited significant oxidation resistance. Nonwoven mats of PND/PMCS polymer composite fibers were readily obtained by the electrostatic spinning of polymer blend solutions. The pyrolytic ceramic conversion reactions of the PND/PMCS polymer fibers then produced mats of micro- and nanodiameter boron-carbide/silicon-carbide ceramic composite fibers.

Introduction

The unique properties of silicon-carbide- and boron-carbide-based ceramics give rise to numerous applications.[1,2] Boron-carbide has high chemical inertness, thermal stability, and hardness and excellent high-temperature thermoelectric properties, whereas silicon carbide is valued because of its low density, high strength, and excellent oxidation and thermal-shock resistance. Boron-carbide/silicon-carbide composites have likewise been shown to have enhanced properties relative to the individual ceramics. For example, although boron carbide oxidizes at ~600 °C to form B_2O_3, boron-carbide/silicon-carbide composites have been reported to have oxidative stability up to 1200 °C as the result of the formation of a borosilicate glass layer that effectively blocks oxygen penetration.[3−5]

Powder processing and sintering techniques are the most common methods of making boron carbide and silicon carbide, but these methods are limited in their ability to produce ceramics in processed forms.[6] More recently, processable polymeric precursors have been developed for both of these ceramics that allow their syntheses in more complex forms, including films and fibers. Nevertheless, the construction of similar single-source precursors for boron-carbide/silicon-carbide composite materials that would allow both for the formation of processed forms and easy tunabilty of composition would be a chemically difficult and expensive challenge. On the other hand, other studies[7−9] have shown that simple mixtures of preceramic polymers can be used to produce ceramic composites. For example, a blend of the polyborazylene[10] and allylhydridopolycarbosilane (AHPCS)[11] preceramic polymers has been used to produce boron-nitride/silicon-carbide composite ceramics. These earlier reports suggested to us that a similar blend strategy might be useful for the formation of boron-carbide/silicon-carbide composites. In this paper, we report that the ceramic conversion reactions of blends of poly(norbornenyldecaborane) (PND) with either poly(methylcarbosilane) (PMCS) or allylhydridopolycarbosilane (AHPCS) provide, in fact, excellent routes to such composites and, in the case of the PND/PMCS blends, enable the electrostatic spinning of composite ceramic fibers.

Experimental Section

Materials. Poly(norbornenyldecaborane) (PND) was synthesized as described previously.[12] Poly(methylcarbosilane) (PMCS) (Aldrich M_w = 3500, electronic grade) and allylhydridopolycarbosilane (AHPCS) (Starfire Systems) were used as received, except that any volatile impurities were removed from the AHPCS by pumping under high vacuum. Methylene chloride and THF (Aldrich) were used as received.

* Corresponding author. E-mail: hra@chem.psu.edu (H.A.); lsneddon@sas.upenn.edu (L.G.S.).
[†] University of Pennsylvania.
[‡] The Pennsylvania State University.

(1) (a) Messier, D. R.; Scroft, W. J. *Preparation and Properties of Solid State Materials*; Wilcox, W. R., Ed.; Marcell Dekker: New York, 1976. (b) Narula, C. K. *Ceramic Precursor Technology and Its Applications*; Marcell Dekker:: New York, 1995.
(2) Thevenot, F. *Key Eng. Mater.* **1991**, *56−57*, 59–88.
(3) (a) Shipilova, L. A.; Petrovskii, V. Y.; Chugunova, S. I. *Powder Metall. Met. Ceram.* **1998**, *36*, 652–656. (b) Narushima, T.; Goto, T.; Maruyama, M.; Arashi, H.; Iguchi, Y. *Mater. Trans.* **2003**, *44*, 401–406.
(4) Guo, Q.; Song, J.; Liu, L.; Zhang, B. *Carbon* **1999**, *37*, 33–40.
(5) Kobayashi, K.; Maeda, K.; Sano, H.; Uchiyama, Y. *Carbon* **1995**, *33*, 397–403.
(6) (a) Thummler, F.; Oberacker, R. *An Introduction to Powder Metallurgy*; Institute of Materials: London, 1993. (b) Singh, M. *Scr. Mater.* **1996**, *34*, 923–927. (c) Chen, Z. F.; Su, Y. C.; Cheng, Y. B. *Key Eng. Mater.* **2007**, *352*, 207–212.
(7) (a) Moraes, K.; Vosburg, J.; Wark, D.; Interrante, L. V.; Puerta, A. R.; Sneddon, L. G.; Narisawa, M. *Chem. Mater.* **2004**, *16*, 125–132. (b) Interrante, L. V.; Moraes, K.; Liu, Q.; Lu, N.; Puerta, A.; Sneddon, L. G. *Pure Appl. Chem.* **2002**, *74*, 2111–2117.
(8) Bao, X.; Edirisinghe, M. J. *Composites, Part A* **1999**, *30*, 601–610.

10.1021/cm900304r CCC: $40.75
Published on Web 04/02/2009

Table 1. Ceramic Conversion Reactions of PND/PMCS Polymer Blends

	PND/PMCS	TGA char yield (%, 1200 °C)	bulk precursor/char (g/g)	bulk ceramic at *T* (°C)	bulk char yield (%)	density (g/cm^3)
1	1.00	84.6	0.22/0.19	1000	86.4	2.08
2	1.00	84.6	0.22/0.16	1300	72.7	2.26
3	1.00	84.6	0.23/0.15	1600	65.2	2.30
4	1.21	86.0	0.28/0.23	1000	82.1	2.14
5	1.21	86.0	0.24/0.18	1300	75.0	2.26
6	1.21	86.0	0.30/0.20	1600	66.7	2.42
7	2.55	82.5	0.31/0.22	1000	71.0	1.81
8	2.55	82.5	0.34/0.23	1300	67.6	2.13
9	2.55	82.5	0.29/0.21	1600	72.4	2.34
10	3.55	82.5	0.20/0.15	1000	75.0	1.78
11	3.55	82.5	0.23/0.16	1300	69.6	2.14
12	3.55	82.5	0.21/0.12	1600	57.1	2.29

Table 2. Ceramic Conversion Reactions of the PND/AHPCS Polymer Blends

	PND/AHPCS	TGA char yield (%, 1200 °C)	bulk precursor/char (g/g)	bulk ceramic at *T* (°C)	bulk char yield (%)	density (g/cm^3)
	AHPCS	73.3	0.67/0.35	1650	52.2	2.54
13	0.22	82.3	0.46/0.28	1650	60.9	2.66
14	0.44	82.6	0.50/0.31	1650	62.0	2.47
15	0.87	83.7	0.49/0.37	1650	75.5	2.33
16	1.21	79.6	0.58/0.41	1650	70.7	2.30
17	2.63	79.1	0.26/0.23	800	89	1.93
18	2.63	79.1	0.40/0.29	1000	73	2.09
19	2.63	79.1	0.46/0.32	1200	70	2.21
20	2.63	79.1	0.39/0.26	1400	67	2.30
21	2.63	79.1	0.53/0.33	1650	62.2	2.32
22	3.63	77.5	0.47/0.29	1650	61.7	2.30
23	4.97	78.0	0.48/0.32	1650	66.7	2.34
	PND	71.1	0.53/0.31	1650	58.5	2.20

Physical Measurements. FTIR measurements for the PND/PMCS blends employed a Perkin-Elmer Spectrum 100, whereas those of the PND/AHPCS blends used a Perkin-Elmer 2000 Spectrometer. Thermogravimetric analyses (TGA) were obtained on a Texas Instruments SDT 2960 Simultaneous DTA-TGA analyzer, using a ramp rate of 10 °C/min up to 1200 °C, under ultra high purity argon gas with a purge rate of 80 mL/min. TGA oxidation experiments were performed under dry breathing air with a ramp rate of 5 °C/min up to 1200 °C. Powder X-ray diffraction (XRD) analyses were obtained on a Rigaku Geigerflex automated X-ray powder diffractometer using Cu Kα radiation and a graphite monochromator. Experimental results and peak assignments are compared to β-SiC (#73−1665) and B_4C (#35−0798) in the JCPDS International Centre for Diffraction Data Database. Scanning electron microscopy (SEM) images were obtained with an FEI Strata DB235 Focused Ion Beam. The samples were gold coated. A working distance of approximately 5−5.5 mm and an accelerating voltage of 20.0 kV were used. Transmission electron microscopic (TEM) images were obtained on a JEOL 2010F. Elemental analyses were performed at the Nesmeyanov Institute of Organoelement Compounds (INEOS), Moscow, Russia.

Polymer Blend Preparations. *PND/PMCS.* In the ratios indicated in Table 1, separate solutions of PND and PMCS were prepared by slowly dissolving each precursor in methylene chloride. The two solutions were combined, stirred, and then sonicated for 20 min. The solvent was removed in vacuo to yield solid orange-brown polymer blends.

PND/AHPCS. In the ratios described in Table 2, separate solutions of PND and AHPCS were prepared by first dissolving each precursor in THF. The two solutions were combined, stirred, and then sonicated for 20 min. Following vacuum evaporation of the THF, the 0.22 PND/AHPCS blend was obtained as a light-yellow oil, but all other compositions were yellow solids.

Bulk Ceramic Conversion Reactions. For all bulk pyrolyses, an aliquot of the polymer blend was weighed by difference into a boron nitride crucible. The crucible was then transferred into a Lindberg model 54434 tube furnace flushed with high-purity argon. After allowing the system to equilibrate for 30 min, the furnace was heated at 5 °C/min to the desired temperature and held there for 1−2 h for the PND/PMCS blends and 8 h for the PND/AHPCS blends before cooling to room temperature. The elemental compositions of the resulting ceramic composites are presented in Tables 3 and 4.

Fiber Electrostatic Spinning Procedures and Fiber Ceramic Conversion Reactions. Two different blend compositions of PND:PMCS were used to produce the fibrous mats: 1.2:1.0 and 2.6:1.0. A general procedure to produce the mats is described as follows: A solution of the polymer blend in dry THF (25% for 1.2:1.0 and 31% for 2.6:1.0 (weight/volume)) was electrostatically spun (potential: 11 kV (1.2:1.0) and 15 kV (2.6:1.0); flow rate: 1.0 mL h^{-1}) to give a nonwoven mat of fine fibers, which was collected on a carbonized Teflon target at a distance of 15 cm. The total weights of the polymer blends used were 458 mg for the 1.2:1.0 mixture and 346 mg for the 2.6:1.0 mixture.

The polymer mats were cut into small pieces and transferred from the carbonized Teflon target into a boron nitride boat. The boat was then transferred into the Lindberg tube furnace flushed with high-purity argon. After allowing the system to equilibrate for 30 min, the furnace was heated at 5 °C/min to the desired temperature and held there for 1−2 h (PND/PMCS) before being cooled to room temperature. The ceramic conversion data for the mats are presented in Table 5.

(9) Garcia, C. B. W.; Lovell, C.; Curry, C.; Faught, M.; Zhang, Y.; Wiesner, U. *J. Polym. Sci., Part B: Polym. Phys.* **2003**, *41*, 3346–3350.
(10) Fazen, P. J.; Remsen, E. E.; Beck, J. S.; Carroll, P. J.; McGhie, A. R.; Sneddon, L. G. *Chem. Mater.* **1995**, *7*, 1942–1956.
(11) (a) Interrante, L. V.; Whitmarsh, C. W.; Sherwood, W.; Wu, H.-J.; Lewis, R.; Maciel, G. *Mater. Res. Soc. Symp. Proc.* **1994**, *346*, 593–603. (b) Interrante, L. V.; Whitmarsh, C. W.; Sherwood, W. *Ceram. Trans.* **1995**, *58*, 111–118.
(12) (a) Wei, X.; Carroll, P. J.; Sneddon, L. G. *Organometallics* **2004**, *23*, 163–165. (b) Wei, X.; Carroll, P. J.; Sneddon, L. G. *Chem. Mater.* **2006**, *18*, 1113–1123.

Table 3. Elemental Compositions of PND/PMCS Polymer Blend Derived Ceramics

	PND/PMCS	*T* (°C)	precursor element ratio	ceramic elemental analysis (%)	Si:B:C (ceramics)	nominal composition
4	1.21	1000	$Si_{1.00}B_{3.25}C_{4.28}$	25.3 Si; 29.4 B; 36.6 C	$Si_{1.0}B_{3.0}C_{3.4}$	$(SiC)_{1.0}(B_4C)_{0.76}C_{1.63}$
5	1.21	1300	$Si_{1.00}B_{3.25}C_{4.28}$	25.8 Si; 32.1 B; 37.8 C	$Si_{1.0}B_{3.0}C_{3.2}$	$(SiC)_{1.0}(B_4C)_{0.75}C_{1.43}$
6	1.34	1500	$Si_{1.00}B_{3.60}C_{4.52}$	26.4 Si; 39.2 B; 32.3 C	$Si_{1.0}B_{3.9}C_{2.9}$	$(SiC)_{1.0}(B_4C)_{0.96}C_{0.84}$
7	2.55	1000	$Si_{1.00}B_{6.80}C_{4.80}$	18.5 Si; 42.4 B; 37.5 C	$Si_{1.0}B_{6.0}C_{4.8}$	$(SiC)_{1.0}(B_4C)_{1.49}C_{2.26}$
8	2.55	1300	$Si_{1.00}B_{6.80}C_{4.80}$	18.3 Si; 42.8 B; 37.4 C	$Si_{1.0}B_{6.1}C_{4.8}$	$(SiC)_{1.0}(B_4C)_{1.52}C_{2.26}$
9	2.55	1600	$Si_{1.00}B_{6.80}C_{4.80}$	18.5 Si; 43.8 B; 37.2 C	$Si_{1.0}B_{6.2}C_{4.7}$	$(SiC)_{1.0}(B_4C)_{1.54}C_{2.17}$
10	3.55	1000	$Si_{1.00}B_{9.54}C_{8.67}$	12.5 Si; 44.6 B; 36.0 C	$Si_{1.0}B_{9.3}C_{6.7}$	$(SiC)_{1.0}(B_4C)_{2.32}C_{3.41}$
11	3.55	1300	$Si_{1.0}B_{9.54}C_{8.67}$	12.4 Si; 47.1 B; 36.1 C	$Si_{1.0}B_{9.9}C_{6.8}$	$(SiC)_{1.0}(B_4C)_{2.47}C_{3.32}$
12	3.60	1550	$Si_{1.0}B_{9.67}C_{8.77}$	12.5 Si; 49.9 B; 32.8 C	$Si_{1.0}B_{10.4}C_{6.16}$	$(SiC)_{1.0}(B_4C)_{2.60}C_{1.13}$

Table 4. Elemental Compositions of PND/AHPCS Polymer Blend Derived Ceramics

	PND/AHPCS	*T* (°C)	precursor element ratio	ceramic elemental analysis (%)	Si:B:C (ceramics)	nominal composition
13	0.22	1650	$Si_{1.0}B_{0.50}C_{1.64}$	59.93 Si; 12.64 B; 22.55 C	$Si_{1.0}B_{0.54}C_{0.88}$	$(SiC)_{0.73}(B_{10.5}C)_{0.05}Si_{0.28}$
14	0.44	1650	$Si_{1.0}B_{0.99}C_{1.99}$	49.49 Si; 17.65 B; 21.36 C	$Si_{1.0}B_{0.92}C_{1.06}$	$(SiC)_{1.0}(B_8C)_{0.06}B_{0.46}$
15	0.87	1650	$Si_{1.0}B_{1.96}C_{2.67}$	39.72 Si; 29.36 B; 27.78 C	$Si_{1.0}B_{1.92}C_{1.63}$	$(SiC)_{1.0}(B_4C)_{0.48}C_{0.15}$
16	1.21	1650	$Si_{1.0}B_{2.72}C_{3.20}$	31.70 Si; 34.53 B; 25.19 C	$Si_{1.0}B_{2.82}C_{1.85}$	$(SiC)_{1.0}(B_4C)_{0.71}C_{0.14}$
17	2.63	800	$Si_{1.0}B_{5.92}C_{5.43}$	18.26 Si; 38.21 B; 32.7 C	$Si_{1.0}B_{5.43}C_{4.18}$	$(SiC)_{1.0}(B_4C)_{0.88}C_{1.19}$
18	2.63	1000	$Si_{1.0}B_{5.92}C_{5.43}$	17.99 Si; 39.14 B; 31.15 C	$Si_{1.0}B_{5.63}C_{4.03}$	$(SiC)_{1.0}(B_4C)_{0.91}C_{1.05}$
19	2.63	1200	$Si_{1.0}B_{5.92}C_{5.43}$	17.97 Si; 42.02 B; 26.62 C	$Si_{1.0}B_{6.05}C_{3.45}$	$(SiC)_{1.0}(B_4C)_{0.97}C_{0.60}$
20	2.63	1400	$Si_{1.0}B_{5.92}C_{5.43}$	20.72 Si; 42.74 B; 31.42 C	$Si_{1.0}B_{5.34}C_{3.53}$	$(SiC)_{1.0}(B_4C)_{0.99}C_{0.89}$
21	2.63	1650	$Si_{1.0}B_{5.92}C_{5.43}$	20.74 Si; 42.72 B; 31.58 C	$Si_{1.0}B_{5.35}C_{3.55}$	$(SiC)_{1.0}(B_4C)_{1.34}C_{1.21}$
22	3.63	1650	$Si_{1.0}B_{8.17}C_{7.00}$	14.81 Si; 48.48 B; 30.40 C	$Si_{1.0}B_{8.62}C_{4.86}$	$(SiC)_{1.0}(B_4C)_{2.16}C_{1.70}$
23	4.97	1650	$Si_{1.0}B_{11.2}C_{9.10}$	13.29 Si; 56.04 B; 23.99 C	$Si_{1.0}B_{11.0}C_{4.25}$	$(SiC)_{1.0}(B_4C)_{2.75}C_{0.50}$

Table 5. Ceramic Conversion Data for PND/PMCS Fibrous Mats Obtained from Electrostatic Spinning

	PND/PMCS	*T* °C	precursor/char (g/g)	char yield (%)
4m	1.20	1000	0.036/0.032	88
5m	1.20	1300	0.041/0.025	61
6m	1.20	1600	0.045/0.032	71
7m	2.60	1000	0.079/0.061	76
8m	2.60	1300	0.052/0.032	61
9m	2.60	1600	0.092/0.022	54

Results and Discussion

As illustrated by eqs 1−3 for their idealized ceramic conversion reactions, poly(norbornenyldecaborane) (PND),[12,13] poly(methylcarbosilane) (PMCS),[14] and allylhydridopolycarbosilane (AHPCS)[11] have previously been shown to be processable precursors to boron-carbide and silicon-carbide ceramic materials.

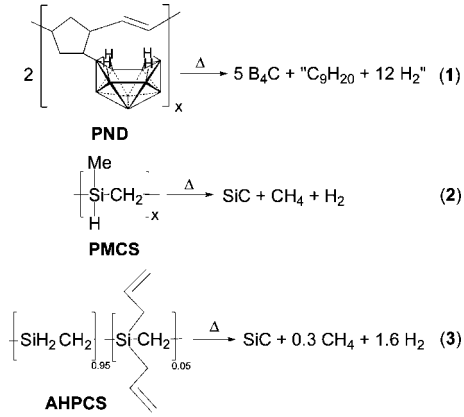

Because of their similar solubilities, PND/PMCS and PND/AHPCS blends of these polymers with a range of compositions (Tables 1 and 2) were easily made from their THF or methylene chloride solutions. The fact that both of the solid polymer blends could be readily redissolved in CH_2Cl_2 (PND/PMCS) and THF (PND/AHPCS) and, additionally, that the FTIR spectra of the blends (Figures 1 and 2) appeared to be additive of their individual components indicates that no significant reaction occurred during their preparations. Likewise, GPC traces of both of the polymer blends in THF using the light scattering detector showed two separate peaks with retention times in accord with their two individual polymers, confirming that only physical mixing rather than chemical reaction occurred in the blending process.

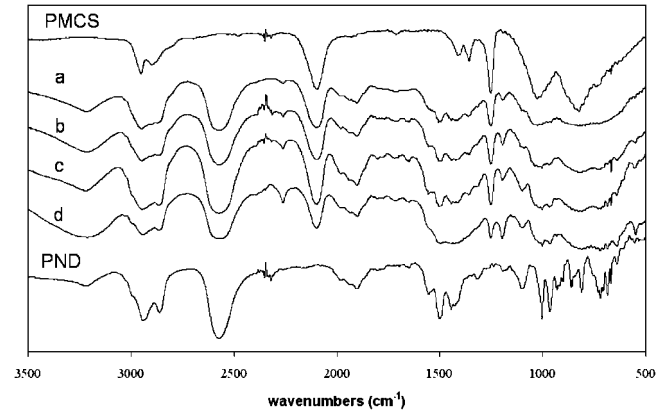

Figure 1. FTIR spectra of PND/PMCS polymer blends with weight ratios of (a) 1.00:1 PND/PMCS, (b) 1.21:1 PND/PMCS, (c) 2.55:1 PND/PMCS, and (d) 3.55:1 PND/PMCS.

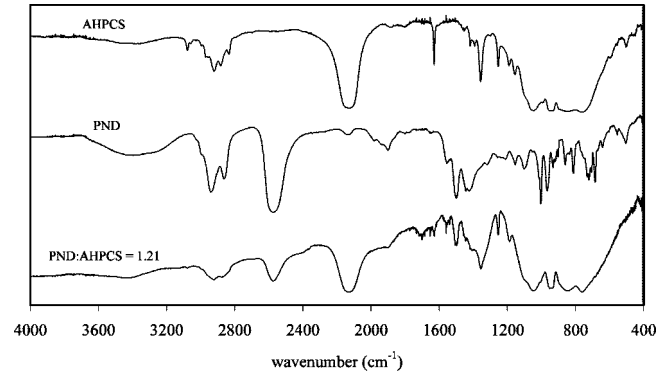

Figure 2. FTIR spectra of AHPCS, PND, and the 1.21 PND/AHPCS blend.

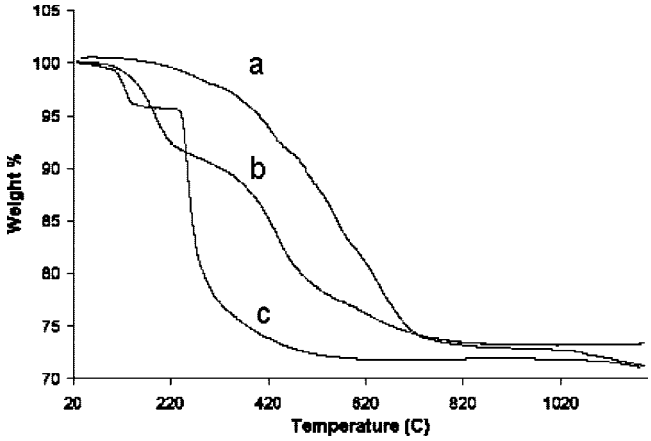

Figure 3. TGA curves (10 °C/min heating rate under high-purity argon) for the ceramic conversion reactions of (a) PMCS, (b) AHPCS, and (c) PND.

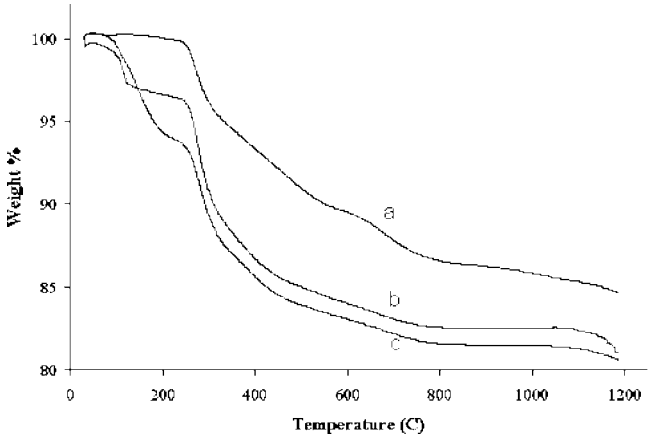

Figure 4. TGA curves (10 °C/min heating rate under high-purity argon) of (a) 1.21:1 PND/PMCS, (b) 3.55:1 PND/PMCS, and (c) 2.55:1 PND/PMCS.

The TGA curves for pure samples of PND, PMCS, and AHPCS are shown in Figure 3. Although the observed 71% char yield for AHPCS is somewhat lower than the 83.3% yield predicted by eq 3, the observed 72% PND and 73% PMCS char yields are higher than their theoretical char yields based on the idealized reactions in eqs 1 and 2, PND (64.5%), PMCS (69.0%), indicating the retention of residual carbon in their derived ceramics. Both PND and AHPCS showed two-step ceramic conversions. PND began weight loss near 150 °C, while AHPCS had its first loss near 230 °C. These were followed by larger weight losses at higher temperatures (PND, beginning near 250 °C; and AHPCS, beginning near 460 °C). On the other hand, PMCS was found to be stable to above 200 °C before undergoing a single-step weight loss that was essentially complete by 800 °C.

TGA analyses of the PND/PMCS and PND/AHPCS blends with different polymer ratios are presented in Figures 4 and 5. The final TGA char yields to 1200 °C for all blend compositions (PND/PMCS, 83−86%; PND/AHPCS, 78−84%) were higher than those of any of the individual polymers, suggesting that effective interpolymer cross-linking reactions occurred during their ceramic conversions. For the PND/PMCS blends, the higher PND ratio materials again showed two-step ceramic conversions with the initial loss beginning at a temperature near that of pure PND. On the other hand,

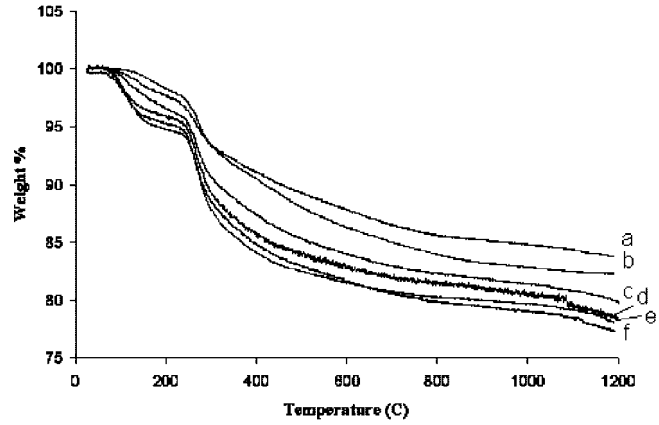

Figure 5. TGA curves (10 °C/min heating rate under high-purity argon) of (a) 0.87:1 PND/AHPCS, (b) 0.44:1 PND/AHPCS, (c) 1.21:1 PND/AHPCS, (d) 2.63:1 PND/AHPCS, (e) 4.97:1 PND/AHPCS, and (f) 3.63:1 PND/AHPCS.

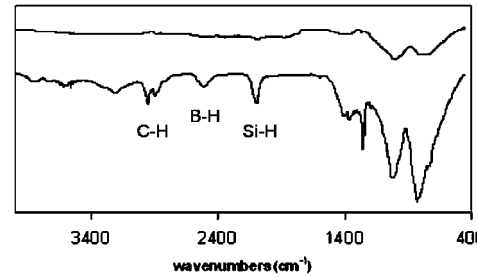

Figure 6. FTIR spectra of the ceramic conversion products of the 1.21:1 PND/PMCS blend after heating at 400 °C (bottom) and 600 °C (top).

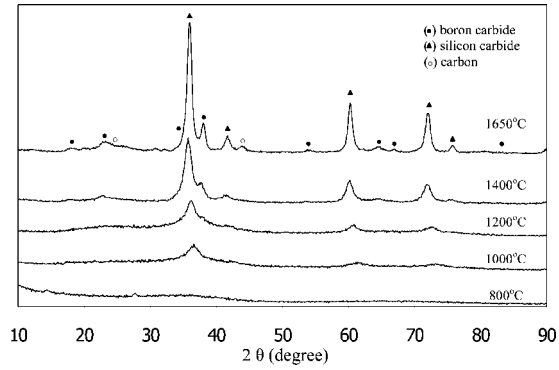

Figure 7. XRD patterns of ceramic chars obtained from the 2.63:1 PND/AHPCS blend at different temperatures: 800 °C (**17**), 1000 °C (**18**), 1200 °C (**19**), 1400 °C (**20**), and 1650 °C (**21**).

the TGA profile of the 1.21:1 PND/PMCS more resembled that of PMCS, showing a good processing window with no weight loss until over 200 °C. IR spectra (Figure 6) of the 1.21:1 blend pyrolyzed to intermediate temperatures showed that B−H and Si−H units were still present at 400 °C, but that these groups were absent at 600 °C.

All of the PND/AHPCS blends exhibited two-step ceramic conversions, with the onset of the initial loss moving to higher temperatures as the PND to AHPCS ratio was decreased. However, even the lowest ratio 0.87:1 PND/AHPCS blend was stable to only ∼175 °C, thus indicating that the PND/AHPCS blends have a much lower thermal processing range than the PND/PMCS blends.

Bulk Ceramic Conversion Reactions. Bulk ceramic conversion reactions were carried out in a tube furnace under

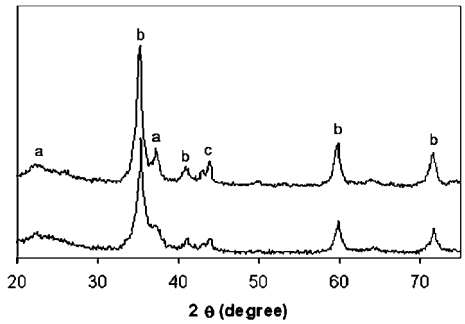

Figure 8. XRD patterns of ceramic chars derived from a 2.55:1 weight ratio PND/PMCS blend at 1300 °C, **8** (bottom), and 1600 °C, **9** (top). Diffraction peaks: (a) boron carbide, (b) silicon carbide, (c) stainless steel holder.

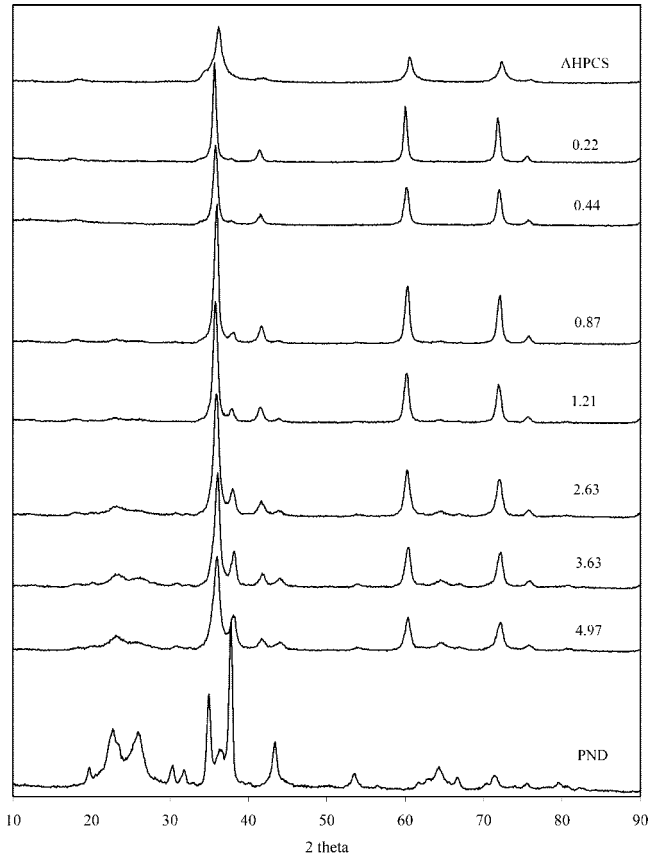

Figure 9. XRD patterns of the 1650 °C chars obtained from blends with different PND/AHPCS ratios.

argon purge. The analytical data in Tables 3 and 4 for the ceramic chars obtained from the pyrolyses of the PND/PMCS and PND/AHPCS blends at different temperatures are consistent with the formation of $SiC/B_4C/C$ composites with the B_4C to SiC ratio in the ceramic increasing as the PND to PMCS and PND to AHPCS ratios were increased in the precursor blends. In all cases, the bulk char yields at 1600 °C (PND/PMCS) and 1650 °C (PND/AHPCS) were 10−20% lower than the TGA yields measured at 1200 °C, but were significantly higher than the bulk char yields we observed for pure samples of the PND (52.2%), PMCS (62.4%), and AHPCS (58.5%) polymers at comparable temperatures.

Previous studies of the ceramic conversion reactions of the PMCS[14] and AHPCS[11] polymers have shown that AHPCS-derived silicon carbide ceramics have much lower residual carbon than those obtained from PMCS. The analytical data for the PND/PMCS- and PND/AHPCS-derived ceramics likewise showed that although significant amounts of carbon were retained in all of the PND/PMCS derived ceramics, there were much smaller amounts of carbon in the PND/AHPCS-derived materials. In fact, no free carbon was found in the ceramics derived from the lowest PND/AHPCS ratios (0.22:1 and 0.44:1).

XRD studies showed that materials obtained from either blend pyrolyzed to only 1000 °C were largely amorphous. However, as shown in the typical XRD patterns presented in Figure 7 for a ceramic derived from a 2.63 PND/AHPCS blend and in Figure 8 for the ceramic derived from a 2.55:1 PND/PMCS blend, the appearance of the three major peaks for β-SiC at $2\theta = 35.7°$ (111), 60.1° (220), and 72.0° (311) indicated that the onset of silicon carbide crystallization occurred by 1200−1300 °C. The onset of boron carbide crystallization, as evidenced by the appearance of its most intense diffraction peak at $2\theta = 37.8°$ (021) was not apparent until after annealing at higher temperatures. As shown in Figure 9, the intensity of the boron carbide diffraction peaks in the 1650 °C ceramics derived from the PND/AHPCS blends increased as the PND to AHPCS ratio increased. On the other hand, there was no clear trend in the relative ratios of the silicon-carbide and boron-carbide diffraction peaks as the PND/PMCS ratio was increased.

The TEM images in Figure 10 from char **8**, which was produced from the 2.55:1 PND/PMCS ratio at 1300 °C, show that this material was composed of nanocrystallites (dark spots with diameter of ∼5−15 nm) embedded in an amorphous matrix (light-colored background). Both the structure of the crystalline pattern and the measured interlayer spacing (0.27 nm) observed in the images of the nanocrystallites are characteristic of β-SiC.[15] The sizes of the nanocrystallites are also consistent with the 14 nm value calculated by the Scherrer equation using the fwhm value of the β-SiC (111) diffraction peak in the pattern in Figure 8. A layered coating, with the measured interlayer spacing (0.35 nm) consistent with that of graphite, was also observed at the boundary of the nanocrystallite and amorphous phases. This graphitic layer encapsulates the β-SiC grains and possibly inhibited their growth.

Density measurements (Tables 1 and 2), carried out by floatation of the ceramic chars in halogenated hydrocarbon solvents, showed that the densities of the ceramics increased at higher temperatures, but with the values for the higher temperature chars still falling below those of pure boron-carbide (2.52 g/cm^3) and silicon carbide (3.21 g/cm^3).

Preliminary Oxidation Studies. Silicon carbide-based materials have good oxidative stability because of the formation at high temperatures of a thin, dense and self-healing protective silica layer at the solid−gas interface. This

(13) (a) Welna, D. T.; Bender, J. D.; Wei, X.; Sneddon, L. G.; Allcock, H. R. *Adv. Mater.* **2005**, *17*, 859–862. (b) Welna, D. T.; Wei, X.; Bender, J. D.; Krogman, N. R.; Sneddon, L. G.; Allcock, H. R. *Mater. Res. Soc. Symp. Proc.* **2005**, *848*, 287–292. (c) Wei, X.; Welna, J. D.; Bender, J. D.; Sneddon, L. G.; Allcock, H. R. *Mater. Res. Soc. Symp. Proc.* **2005**, *848*, 37–42.
(14) Yajima, S. *Am. Ceram. Soc. Bull.* **1983**, *62*, 893–898.
(15) Jepps, N. W.; Smith, D. J.; Page, T. F. *Acta Crystallogr., Sect. A* **1979**, *35*, 916–923.

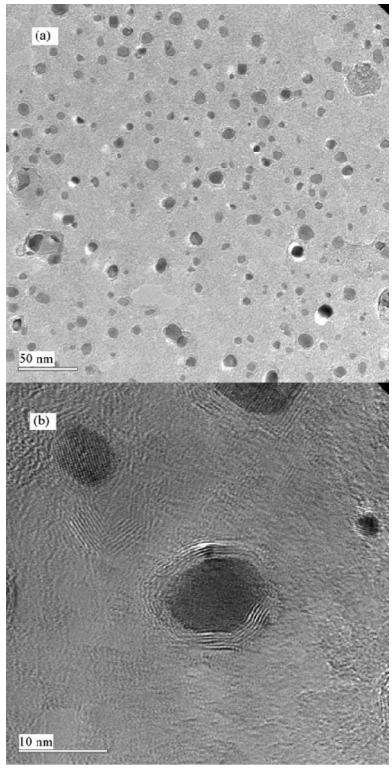

Figure 10. (a) Low- and (b) high-resolution TEM images of the ceramic char **8**, obtained from a 2.55:1 weight ratio PND/PMCS blend pyrolyzed to 1300 °C, showing silicon-carbide crystallites embedded in an amorphous boron-carbon phase.

layer impedes oxygen permeation into the bulk substrate and thus prevents further oxidation.[16] For SiC/B_4C/C composites, Kobayashi,[5] Zhang,[17] and Guo[4] proposed that initially boron will oxidize to form a surface B_2O_3 layer at lower temperatures (<800 °C). This B_2O_3 layer inhibits oxygen permeation and further oxidation at these lower temperatures. At temperatures >900 °C, some of the B_2O_3 will evaporate, allowing silicon to oxidize and form a SiO_2 layer that provides another barrier for oxygen permeation. Additionally, the SiO_2 can also react with B_2O_3 to form a glassy borosilicate surface layer, which because of its low volatility and oxygen permeability can provide a "self-healing" protective layer that can flow to seal any layer defects. The combination of B_2O_3, SiO_2, and borosilicate can thus potentially provide oxidation protection over a range of temperatures.

Preliminary studies of the oxidative behaviors of the polymer blend-derived SiC/B_4C/C composites were carried out in a TGA under flowing dry breathing air. As shown in Figure 11, the PND/PMCS derived ceramics showed poor oxidation properties, each rapidly oxidizing near 600 °C with the observed weight gain arising from the formation of B_2O_3.

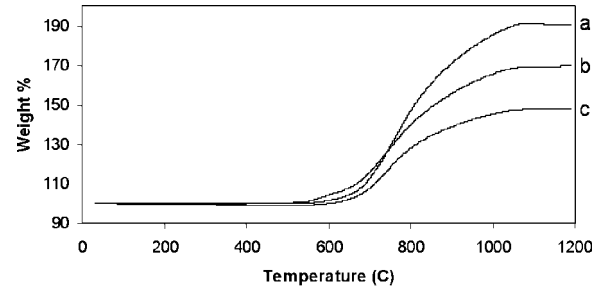

Figure 11. TGA curves under dry breathing air of the ceramics derived from (a) 2.55:1 PND/PMCS, (b) 3.55:1 PND/PMCS, and (c) 1.00:1 PND/PMCS.

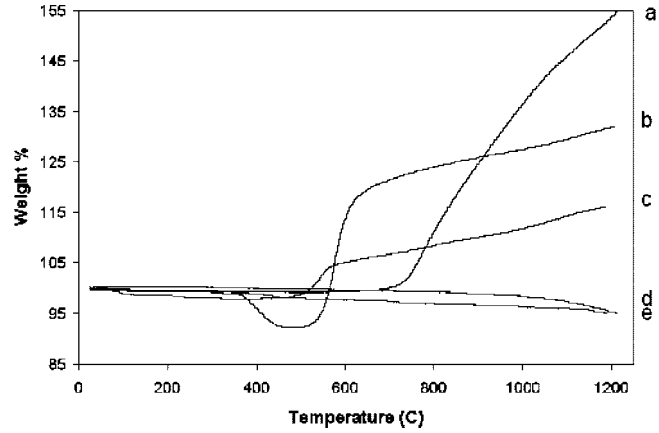

Figure 12. Overlap of TGA curves under dry breathing air of (a) commercial boron carbide, and the 1650 °C ceramic chars derived from (b) PND; (c) 2.63:1 PND/AHPCS, **21**; (d) 1.21:1 PND/AHPCS, **16**; and (e) AHPCS.

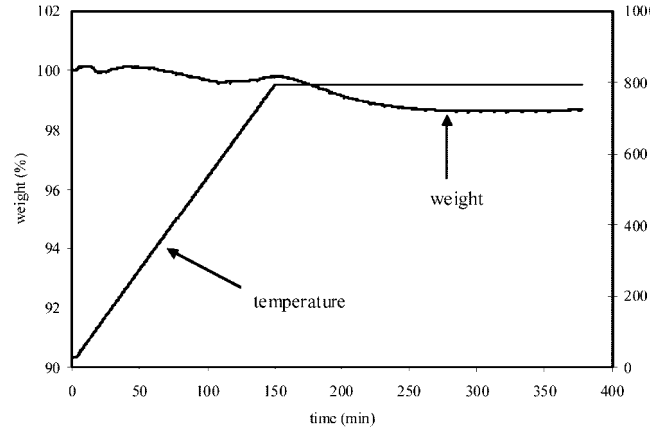

Figure 13. TGA curve of char **13** under dry breathing air at 800 °C (10 °C/min to 800 °C, then held).

On the other hand, many of the 1650 °C ceramic chars derived from PND/AHPCS showed good oxidative resistance (Figure 12) with all of the composites more oxidatively stable than either commercial (curve a) or PND-derived (curve b) boron carbide. Those materials with the highest silicon carbide and lowest free carbon contents showed the best oxidation resistance. For instance, the weights of char **13** and **16**, obtained from the 0.22 PND/AHPCS and 1.21:1 PND/AHPCS blends, respectively, remained essentially constant up to 1200 °C.

Extended time oxidation studies of char **13** at constant temperatures also revealed significant oxidative resistance.

(16) (a) Fox, D. S. *J. Am. Ceram. Soc.* **1998**, *81*, 945–950. (b) Simon, L.; Kubler, L.; Ermolieff, A.; Billon, T. *Microelectron. Eng.* **1999**, *48*, 261–264. (c) Virojanadara, C.; Johansson, L. I. *Surf. Sci.* **2001**, *472*, 145–149. (d) Vickridge, I. C.; Trimaille, I.; Ganem, J.-J.; Rigo, S.; Radtke, C.; Baumvol, I. J. R.; Stedile, F. C. *Phys. Rev. Lett.* **2002**, *89*, 256102/1−256102/4. (e) Colomban, P.; Gouadec, G.; Mazerolles, L. *Mater. Corros.* **2002**, *53*, 306–315. (f) Shimoo, T.; Morisada, Y.; Okamura, K. *J. Am. Ceram. Soc.* **2003**, *86*, 838–845.

(17) Zhang, W. G.; Cheng, H. M.; Sano, H.; Uchiyama, Y.; Kobayashi, K.; Zhou, L. J.; Shen, Z. H.; Zhou, B. L. *Carbon* **1998**, *36*, 1591–1595.

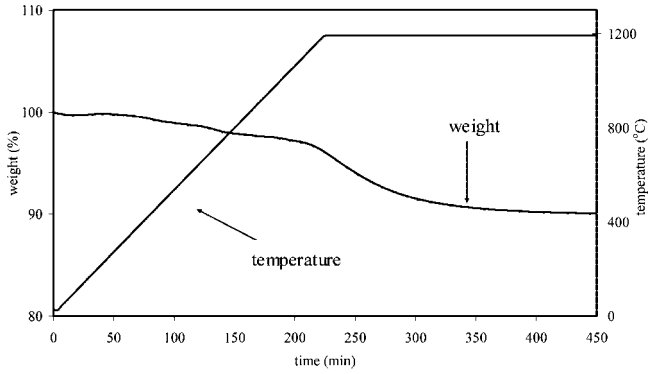

Figure 14. TGA curve of char **13** under dry breathing air at 1200 °C (10 °C/min to 1200 °C, then held).

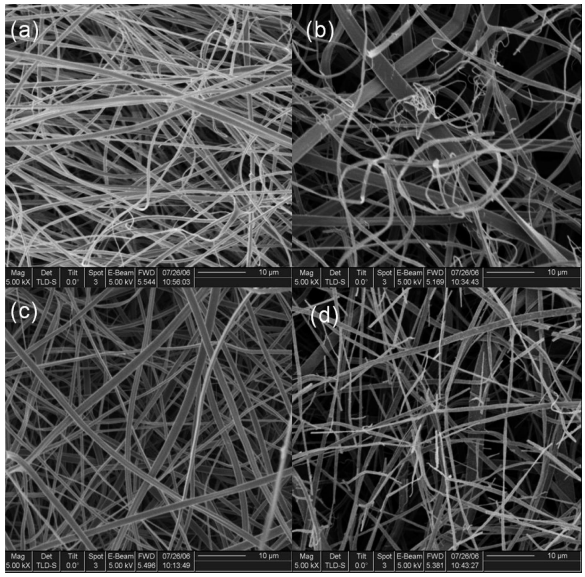

Figure 15. SEM images of fiber mats obtained from a 2.55:1 PND:PMCS blend: (a) polymer fibers and the boron-carbide/silicon-carbide ceramic fibers obtained by pyrolysis at (b) 1000, (c) 1300, and (d) 1600 °C.

For example, as shown in Figure 13, char **13** showed only a 2% weight loss after oxidation at 800 °C for 300 min, with no further change up to 400 min. Likewise, when **13** was treated with air for 325 min at 1200 °C, the weight decreased ~10%, but then remained constant over the next 125 min (Figure 14). The observed weight loss at this temperature is again consistent with the volatilization of B_2O_3. SEM studies of samples after the 800 and 1200 °C oxidations revealed smooth surfaces, consistent with the formation of the glassy silica or silica/borosilicate coatings that have previously been proposed to provide oxidation barriers for silicon-carbide/boron-carbide materials.[4,5,16,17]

Generation of Boron-Carbide/Silicon-Carbide Ceramic Fibers via the Electrostatic Spinning of PND/PMCS and PND/AHPCS Blends. While electrostatic spinning[18] of polymeric precursors, followed by pyrolysis, has now been shown to be an efficient and simple method to prepare fine fibers of carbon,[19] silica,[20] alumina-borate,[21] titania,[22] alumina,[23] niobium oxide,[24] zirconium carbide,[25] and some composite fibers,[26] our recent report[13] of the electrostatic spinning of the PND polymer and the subsequent conversion of the PND polymer fibers to boron-carbide/carbon fibers was the first use of this technique to prepare nonoxide ceramic fibers. The inability to electrostatically spin other

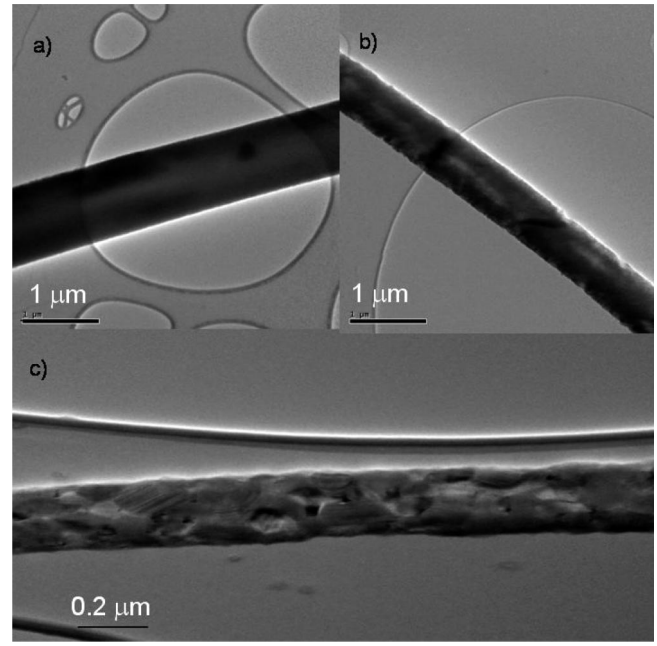

Figure 16. TEM images of 2.55:1 PND:PMCS fibers pyrolyzed to (a) 1000 °C, **7m**; (b) 1300 °C, **8m**; and (c) 1600 °C, **9m**.

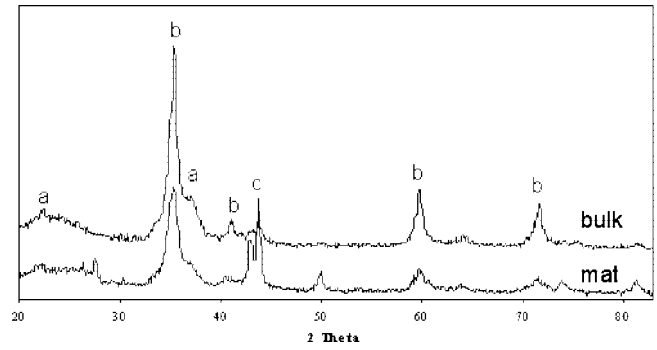

Figure 17. Comparison of the XRD patterns of the 1300 °C chars of the bulk, **8** (top), and electrostatically spun polymer mats, **8m** (bottom), of a 2.55:1 PND/PMCS blend. Diffraction peaks: (a) boron carbide, (b) silicon carbide, and (c) stainless steel holder.

(18) For general references on the use of electrostatic spinning to produce ceramic fibers, see (a) Fong, H. In *Polymeric Nanostructures and Their Applications*; Nalwa, H. S., Ed.; American Scientific Publishers: Stevenson Ranch, CA, 2007; Vol. 2, pp 451−474. (b) Ramaseshan, R.; Sundarrajan, S.; Jose, R.; Ramakrishna, S. *J. Appl. Phys.* **2007**, *102*, 111101/1−111101/17. (c) Li, D.; McCann, J. T.; Xia, Y.; Marquez, M. *J. Am. Ceram. Soc.* **2006**, *89*, 1861–1869. (d) Sigmund, W.; Yuh, J.; Park, H.; Maneeratana, V.; Pyrgiotakis, G.; Daga, A.; Taylor, J.; Nino, J. C. *J. Am. Ceram. Soc.* **2006**, *89*, 395–407.

(19) Wang, Y.; Serrano, S.; Santiago-Aviles, J. J. *Synth. Met.* **2003**, *138*, 423–427.
(20) Shao, C.; Kim, H.; Gong, J.; Lee, D. *Nanotechnology* **2002**, *13*, 635–637.
(21) Dai, H.; Gong, J.; Kim, H.; Lee, D. *Nanotechnology* **2002**, *13*, 674–677.
(22) (a) Li, D.; Xia, Y. *Nano. Lett.* **2003**, *3*, 555–560. (b) Li, D.; Xia, Y. *Polym. Prepr. (Am. Chem. Soc., Div. Polym. Chem.)* **2003**, *44*, 65–66.
(23) Larsen, G.; Velarde-Ortiz, R.; Minchow, K.; Barrero, A.; Loscertales, I. G. *J. Am. Chem. Soc.* **2003**, *125*, 1154–1155.
(24) Viswanathamurthi, P.; Bhattarai, N.; Kim, H. Y.; Lee, D. R.; Kim, S. R.; Morris, M. A. *Chem. Phys. Lett.* **2003**, *374*, 79–84.
(25) Cui, X. M.; Nam, Y. S.; Lee, J. Y.; Park, W. H. *Mater. Lett.* **2008**, *62*, 1961–1964.
(26) Li, D.; Herricks, T.; Xia, Y. *Appl. Phys. Lett.* **2003**, *83*, 4586–4588.

nonoxide preceramic polymers has undoubtedly been a result of their low molecular weights and/or low viscosities. Because of its higher molecular weight (30 KDa), the PND polymer is thus unique in its ability to undergo electrostatic spinning. We have now also found that PND/PMCS blends can be readily electrostatically spun to form nonwoven mats of composite polymer fibers.

As described in the experimental section, THF solutions of the 1.2:1.0 and 2.6:1.0 PND/PMCS blends were readily electrostatically spun to produce 8 cm × 10 cm nonwoven mats of fine polymer-blend fibers. The polymer mats were easily peeled from the collector, cut into smaller pieces and then placed into a boron nitride boat that was transferred to the tube furnace. Pyrolytic ceramic conversion using the conditions described in Table 5 then converted the light-tan polymer mats into black ceramic-composite mats. Because of the smaller sample size, measurements of the char yields of the mats are less precise, but the values in the Table 5 are still in general agreement with those values from the bulk studies.

The SEM images in Figure 15 of mats of ceramic fibers obtained from a 2.55:1 PND/PMCS blend by pyrolysis at (b) 1000, (c) 1300, and (d) 1600 °C confirm that the fiber structure has been retained following ceramic conversion of the polymeric blend fibers (a). As can be seen in the TEM images in Figure 16, the 1000 °C ceramic fibers had a smooth amorphous-like surface structure but also show that significant surface roughening occurred as the annealing temperature was increased to 1300 and 1600 °C. The XRD patterns of the composite ceramic fibers were found to closely match those obtained from the bulk ceramic conversions. For example, as can be seen in the XRD patterns in Figure 17 that were obtained from the 1300 °C chars of bulk and electrostatically spun mats of a 2.6:1 PND/PMCS blend, both materials showed at this stage the formation of β-SiC crystallites, but that the boron-carbide was still amorphous.

In summary, silicon-carbide/boron-carbide composite ceramics can now be easily prepared using simple blends of the poly(norbornenyldecaborane) (PND) boron-carbide preceramic polymer with either of the commercial poly(methylcarbosilane) (PMCS) or allylhydridopolycarbosilane (AHPCS) silicon-carbide precursor polymers. Furthermore, the PND/PMCS and PND/AHPCS blends provide access to composite ceramics with different and controlled compositions and properties. As illustrated by our initial oxidation and fiber spinning studies, this flexibility may provide significant advantages for the tuning of ceramic properties to fit the requirements for a range of potential applications.

Acknowledgment. At the University of Pennsylvania, we thank the Air Force Office of Scientific Research (FA9550-06-1-0228) for support of this project. We also thank Steven Szewczyk for his assistance.

CM900304R